Four-body Scattering Dynamics with Regularized Contact Interactions

Sourav Mondal,* Rakshanda Goswami,† and Udit Raha‡
Department of Physics, Indian Institute of Technology Guwahati, Guwahati-781039, India

Johannes Kirscher§
Department of Physics, SRM University–AP,
Amaravati 522502, Andhra Pradesh, India

1. Introduction

In four-body scattering with two protons and two neutrons, two- and three-body threshold structures significantly influence the system. Universal properties emerge when the effective range of two-body interaction is much smaller than the system length scale. While tuning two-body scattering length is possible in cold-atom experiments, it's challenging in nuclear systems. This study examines the impact of varying the two-body scattering length and adjusting the three-nucleon interaction (TNI), with potential implications for optimizing nuclear fusion rates and improving reaction yields.

2. Theory

The leading-order interaction Hamiltonian in effective field theory for few-body atomic and nuclear systems can be expressed as:

$$H^{(0)}_{int} = \sum_{\{i,j\}} V_2(r_{ij}, \lambda) + \sum_{\{i,j,k\}} V_3(r_{ij}, r_{ik}, \lambda) \tag{1}$$

where T_1 is the one-particle kinetic energy, V_2 is the two-body potential, and V_3 is the three-body potential. The parameter λ distinguishes between various potential forms, all of which yield a two-body system near unitarity.

For numerical methods, interactions are:

$$V_2 = c(\lambda)e^{-\lambda|r_i - r_j|^2}, \tag{2}$$

$$V_3 = d(\lambda)e^{-\lambda(|r_i - r_j|^2 + |r_i - r_k|^2)}, \tag{3}$$

with λ as a cutoff. The scattering length a is large compared to the interaction range $r \sim \lambda^{-1}$. The system approaches unitarity by adjusting two-body binding energies $B_0(2) \to 0$.

3. Results and Discussions

Using a regularized 3-parameter contact interaction with variational methods, we study observables from the multi-channel scattering matrix as functions of (i) the cutoff λ, (ii) bound trimer energies $B_n(3)$, and (iii) dimer binding energy $B_0(2)$.

The observables show minimal dependence on λ within 6 fm$^{-2} \leq \lambda \leq 10$ fm^{-2}. In scenarios (2) and (3), both dimer-dimer ($a^{(0)}_{22}$) and trimer-atom ($a^{(1)}_{31}$) scattering lengths are moderate, while in scenario (1), the large $a^{(0)}_{22}$ may indicate an isolated pole, consistent with the universal ratio found in [1], despite expected deviations in non-unitary cases.

In scenario (2), with weaker TNI than (1), both $a^{(0)}_{22}$ and $a^{(1)}_{31}$ decrease until scenario (4) is reached, where they diverge, and their ratio $\zeta \approx 2$. Further attraction only causes divergence when a third trimer bound state appears, returning to scenario (1). The number of 3-body bound states does not impact the scattering matrix, preserving discrete scale invariance.

*Electronic address: sm206121110@iitg.ac.in
†Electronic address: r.goswami@iitg.ac.in
‡Electronic address: udit.raha@iitg.ac.in
§Electronic address: johannes.k@srmap.edu.in

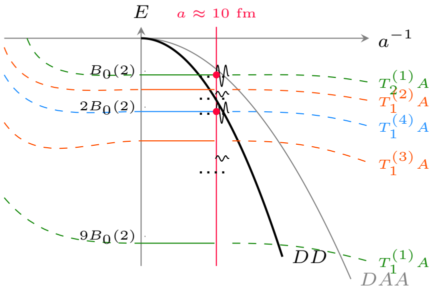

FIG. 1: Dependence of 4-body thresholds on the 2-body scattering length a. For $a = 10$ fm (vertical red line), the gap between dimer-dimer (DD, black) and dimer-atom-atom (DAA, gray) is ≈ 0.5 MeV. Four scenarios are shown: (1) a 2$^{\text{nd}}$ excited state at DAA with a 1$^{\text{st}}$ excited state at ≈ -4.5 MeV (green); (2) the 1$^{\text{st}}$ excited trimer between DAA and DD (orange); (3) the trimer below DD (orange); (4) the trimer at DD. Scenarios (1) and (4) show a diverging trimer-atom scattering length correlated with an isolated 4-body pole (black dotted), while (2) does not, indicating a larger gap to the $T_1^{(2)}A$ threshold.

TABLE I: Cutoff dependence (in fm^{-2}) of dimer-dimer ($a_{22}^{(0)}$) and trimer-atom ($a_{31}^{(1)}$) scattering lengths (both in fm) for a range of $B_1(3)$ renormalization conditions (($\star$)).

λ	$B_1(3)$	$B_0(3)$	$B_0(4)$	$a_{22}^{(0)}$	$a_{31}^{(1)}$
6	1.20	28.0	84.6	21.0(20)	-19.0(20)
	1.32	38.8	120.6	19.0(15)	-3.7(6)
	1.50	63.0	211.4	16.5(15)	3.9(11)
	1.92	119.2	516.7	4.5(5)	-0.8(16)
	5.96	835.2	6457.8	7.1(2)	-8.9(15)
	9.00	1196.6	9132.44	4.5(2)	-12(16)
8	1.20	27	84.8	21.6(19)	-19.7(27)
	1.30	38.8	121.4	20.5(11)	2.1(11)
	1.50	63.4	209.8	15.3(17)	4.6(9)
	1.92	237	473.2	2.5(5)	-0.3(17)
	6.08	928.	7139.6	6.9(2)	-9.4(11)
	8.98	1366.0	10488.6	3.8(2)	-10.1(18)
10	1.22	28.8	90.6	21.5(25)	-21.0(30)
	1.30	37.6	120.0	20.8(17)	-1.1(14)
	6.22	1011.6	7952.4	6.8 (2)	-9.4(9)
	9.04	1510.0	11670.6	3.3(3)	-10(15)

For reactions, the cross section $\sigma_{i\to f}(E)$ is given by:

$$\sigma_{i\to f}(E) = \frac{\pi}{2\mu E} \sum_{J^\pi} \frac{2J+1}{(2s_1+1)(2s_2+1)} \times \sum_{\substack{l_i,l_f \\ s_i,s_f}} \left| S_{i\to f}\left(E, l_{i/f}, s_{i/f}, J\right)\right|^2 \quad (4)$$

where transition cross sections in scenarios (2) and (3) are significantly smaller than elastic cross sections. In scenario (4), where $\zeta \approx 2 \pm \epsilon$ with $\epsilon \ll 1$, the transition cross section can approach the elastic cross section right before the new channel opens. This symmetric behavior contrasts with findings in [2], possibly due to differences in 3-body parameters affecting trimer energy in the unitary limit.

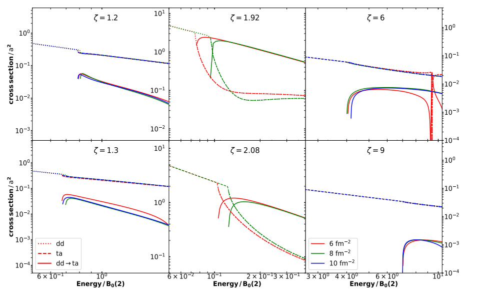

FIG. 2: Reaction ($\sigma_{dd\to ta}$, solid) and elastic ($dd \to dd$ (dotted), $ta \to ta$ (dashed)) cross sections for trimer binding energies below ($B_1(3) < 2\,B_0(2)$, left), at ($B_1(3) \approx 2\,B_0(2)$, middle), and above ($B_1(3) > 2\,B_0(2)$, right) the dimer-dimer threshold. Results are for cutoffs $\lambda = 6$ (red), 8 (green), and 10 (blue) with $B_0(2) = 0.5$ MeV. Energy E is relative to the lowest threshold.

References

[1] A. Deltuva, Efimov physics in bosonic atom-trimer scat- tering, Physical Review A—Atomic, Molecular, and Opti- cal Physics **82** , 040701 (2010).

[2] A. Deltuva, Universality in bosonic dimer-dimer scatter- ing, Physical Review A—Atomic, Molecular, and Optical Physics **84**, 022703 (2011).